Academic Journal of Science and Technology
ISSN: 2771-3032 | Vol. 21, No. 3, 2026

Land-use and Fractional Vegetation Cover Changes in Tianshui, China: Spatiotemporal Patterns and Spatial Associations

Xiaoli Shao, Zhanfu Luo*

College of Geography and Environmental Science, Northwest Normal University, Lanzhou 730070, China
* Corresponding author: Zhanfu Luo (Email: luozhanfu@nwnu.edu.cn)

Abstract: To clarify the spatial association between land-use change and fractional vegetation cover (FVC) dynamics, we integrated land-use and MODIS NDVI data from 2000, 2007, 2015, and 2022 with land-use dynamic degree, land-use transition matrices, the pixel dichotomy model, FVC transition matrices, and spatial overlay analysis to examine the spatiotemporal evolution of land use and FVC in Tianshui from 2000 to 2022. The results showed that (1) land-use structure changed markedly during the study period. Cropland declined by 1,425.795 km², whereas grassland, forest land, and built-up land generally expanded, with the largest increases occurring in grassland and forest land. Land-use conversions occurred mainly among cropland, grassland, and forest land, and built-up land expansion was driven primarily by the conversion of cropland and grassland. (2) FVC generally increased, with higher values in the southeast and lower values in the northwest. Areas of low and relatively low FVC contracted, whereas moderate- and high-FVC areas expanded, indicating an overall shift towards higher FVC classes. (3) Land-use type was closely associated with the spatial distribution of FVC, and vegetation-cover characteristics differed among land-use types. FVC was generally higher in forest land and grassland than in built-up land and unused land. These findings indicate that ecological restoration and land-use adjustment jointly shaped the surface ecological environment of Tianshui and provide a scientific basis for regional land-resource optimization, ecological conservation, and sustainable development.

Keywords: Land use; fractional vegetation cover; spatiotemporal evolution; transition matrix; spatial association.

1. Introduction

Land-use and vegetation-cover changes are important components of research on global environmental change and sustainable development [1]. Land-use change reshapes land-cover structure and affects regional hydrological cycles, energy exchange, biogeochemical processes, and ecosystem services [2]. Land systems provide the spatial basis for food production, settlements, infrastructure, and socioeconomic activities [3]. Land-use and land-cover changes are driven by interacting demographic, economic, institutional, technological, and environmental factors [4]. Continued urbanization converts agricultural and natural land into built-up land and exerts both direct and indirect effects on regional vegetation growth [5]. Vegetation participates in carbon, water, and energy exchanges within terrestrial ecosystems and provides important feedbacks to global environmental change [6]. Fractional vegetation cover (FVC), defined as the proportion of green vegetation covering the land surface, is an important biophysical parameter for monitoring vegetation conditions and ecological change [7]. Therefore, jointly examining land-use and vegetation-cover changes can help reveal interactions between human activities and ecosystems and provide a scientific basis for coordinating land development and ecological conservation.

Long-term remote-sensing records have enabled the global-scale reconstruction of land-use and land-cover change, revealing substantial changes in cropland, forest land, and built-up land over recent decades [10]. At regional scales, remote sensing has been used to identify relationships among land-use patterns, land-surface temperature, and vegetation abundance [11]. These studies demonstrate that land-use transitions not only alter surface spatial patterns but also affect regional thermal conditions, vegetation structure, and ecological processes. Remote-sensing monitoring, geographic information system analysis, land-use transition matrices, and spatial overlay analysis have consequently become important methods for characterizing the spatiotemporal dynamics and ecological implications of land-use change.

NDVI-based spectral mixture models have been widely used to estimate FVC [7]. Among these methods, the pixel dichotomy model estimates FVC by representing a mixed pixel as a combination of vegetation and non-vegetation components [7]. A comprehensive review further summarized the principal algorithms and application conditions for estimating FVC using vegetation-index endmember values [8]. More recently, the accuracy of NDVI mixture models has been improved by accounting for shaded vegetation and soil components [9]. Long-term satellite observations have shown that afforestation and agricultural management in China have contributed substantially to global greening [12]. However, large-scale vegetation restoration may also be constrained by regional water-resource availability [13]. Nevertheless, existing studies have generally examined land-use transitions and vegetation trends separately, while the spatial correspondence between land-use conversions and transitions among different FVC classes remains insufficiently understood.

Tianshui City is located in southeastern Gansu Province, in the transitional zone between the Loess Plateau and the Western Qinling Mountains [14]. The region is characterized by complex loess landforms, mountainous terrain, and pronounced topographic relief [15]. Against this background, systematically assessing land-use and vegetation-cover changes is necessary to understand their spatial associations and ecological implications. Using land-use and NDVI data for 2000, 2007, 2015, and 2022, this study integrates land-use dynamic degree, land-use transition matrices, the pixel dichotomy model, FVC transition matrices, and spatial overlay analysis to examine the spatiotemporal evolution and spatial associations of land use and FVC in Tianshui. The findings provide a scientific basis for territorial spatial planning, sustainable land use, and regional ecological governance.

2. Data Sources and Methodology

2.1. Study area

Tianshui is located in southeastern Gansu Province, along the upper reaches of the Wei River. It borders Baoji in Shaanxi Province and Dingxi, Pingliang, and Longnan in Gansu Province and covers approximately 14,300 km². The city comprises 113 township-level administrative units, including 46 towns, and had 2.9072 million permanent residents in 2023 according to the Tianshui Statistical Communiqué on National Economic and Social Development. Administratively, Tianshui comprises the Qinzhou and Maiji districts; Gangu, Wushan, Qin'an, and Qingshui counties; Zhangjiachuan Hui Autonomous County; and the Tianshui Economic and Technological Development Zone. Tianshui is regarded as one of the cradles of the Chinese nation and civilization. It was among the first places in China to be designated a National Historical and Cultural City and is widely known as the "Hometown of Emperor Fuxi" (Fig. 1).

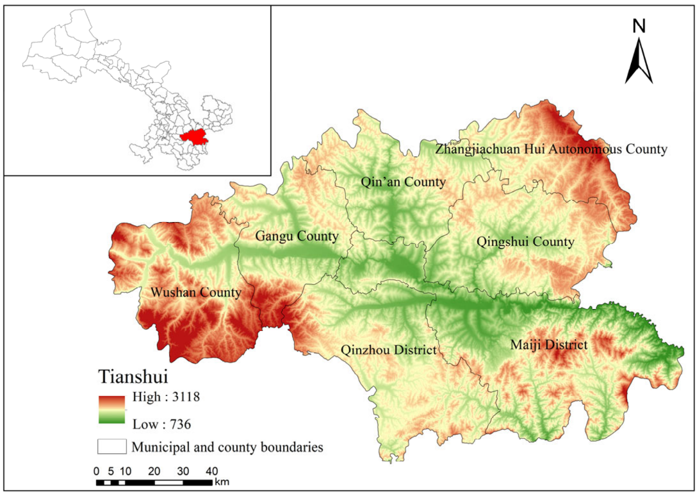

Figure 1. Overview of the study area

2.2. Data sources and preprocessing

The digital elevation model (DEM) was obtained from the Geospatial Data Cloud, whereas administrative boundary data were obtained from the National Earth System Science Data Center. Land-use data for 2000, 2007, 2015, and 2022 were obtained from the annual China Land Cover Dataset (CLCD) produced by Wuhan University. According to the *Current Land Use Classification* standard (GB/T 21010–2017) and the land-use characteristics of the study area, land use was reclassified into six primary categories: grassland, cropland, forest land, water bodies, built-up land, and unused land. MOD13A3 vegetation-index data for the same years were obtained from the Moderate Resolution Imaging Spectroradiometer (MODIS) archive of the National Aeronautics and Space Administration (NASA) at a spatial resolution of 1 km.

The DEM tiles covering Tianshui were mosaicked in ArcGIS and extracted using the administrative boundary as a mask. To ensure consistent spatial accuracy and facilitate subsequent analyses, the CLCD data were reclassified and converted from raster to polygon format in ArcGIS. The area of each land-use category was then calculated from the polygon geometry.

The MOD13A3 images were preprocessed using the MODIS Reprojection Tool (MRT) through batch mosaicking, reprojection, and format conversion. Annual NDVI datasets were generated using the maximum value composite method, clipped to the Tianshui boundary, and reclassified. The processed data were then used to produce fractional vegetation cover (FVC) maps for each study year.

2.3. Methodology

2.3.1. Land-use dynamic degree

Land-use dynamic degree comprises single and comprehensive land-use dynamic degrees. The single land-use dynamic degree quantifies the change in the area of a specific land-use type over a defined period and reflects the intensity of that change. The comprehensive land-use dynamic degree, denoted by L_c, measures the overall intensity of land-use change within the study area [16]. The two indices were calculated as follows:

$$K = \frac{U_{b-}U_a}{U_a} \times \frac{1}{T} \times 100\% \tag{1}$$

$$L_c = \frac{\sum_{i=1}^{n} \Delta LU_{i-j}}{2\sum_{i=1}^{n} LU_i} \times \frac{1}{T} \times 100\% \tag{2}$$

whereU_a and U_b denote the area of a given land-use type at the beginning and end of the study period, respectively; T denotes the duration of the study period in years; K represents the mean annual rate of change in that land-use type; LU_i denotes the area of land-use type i at the beginning of the study period; ΔLU_{i-j} denotes the area converted from land-use type i to other land-use types during the study period; n denotes the number of land-use types; and L_c represents the mean annual rate of overall land-use change within the study area.

2.3.2. Land-use transition matrix

A land-use transition matrix was used to characterize the land-use structure and quantify the direction and magnitude of conversions among land-use types during the study period, thereby identifying the sources and destinations of land-use changes [17]. The matrix is expressed as follows:

$$S_{ij} = \begin{pmatrix} S_{11} & S_{12} & \cdots & S_{1j} & \cdots & S_{1n} \\ S_{21} & S_{22} & \cdots & S_{2j} & \cdots & S_{2n} \\ \vdots & \vdots & \vdots & \vdots & \vdots & \vdots \\ S_{i1} & S_{i2} & \cdots & S_{ij} & \cdots & S_{in} \\ \vdots & \vdots & \vdots & \vdots & \vdots & \vdots \\ S_{n1} & S_{n2} & \cdots & S_{nj} & \cdots & S_{nn} \end{pmatrix} \quad (3)$$

where S_{ij} denotes the area converted from land-use type i to land-use type j during the study period; $i,j = 1,2,\cdots,n$; and n denotes the number of land-use types.

2.3.3. Pixel dichotomy model

The pixel dichotomy model assumes that each pixel consists of vegetation and non-vegetation components, with its observed NDVI representing their combined contributions. Fractional vegetation cover (FVC) was calculated as follows [7]:

$$FVC = \frac{NDVI - NDVI_{soil}}{NDVI_{veg} - NDVI_{soil}} \quad (4)$$

where FVC is fractional vegetation cover; $NDVI$ is the NDVI value of a given pixel; and $NDVI_{veg}$ and $NDVI_{soil}$ are the NDVI values of pure vegetation and bare soil, respectively [8].

3. Result

3.1. Analysis of land-use and fractional vegetation cover changes in Tianshui

3.1.1. Spatiotemporal changes in land use

Based on land-use data for 2000, 2007, 2015, and 2022, land-use distribution maps were generated in ArcGIS 10.7 (Fig.2). Figure 2 and Table 1 indicate substantial changes in land use across Tianshui during 2000–2022. Cropland accounted for the largest proportion of the study area, whereas unused land accounted for the smallest. Forest land, grassland, and built-up land expanded progressively, whereas cropland declined following the implementation of policies promoting the conversion of cropland to forest and grassland. Water bodies also expanded but remained a minor land-use type.

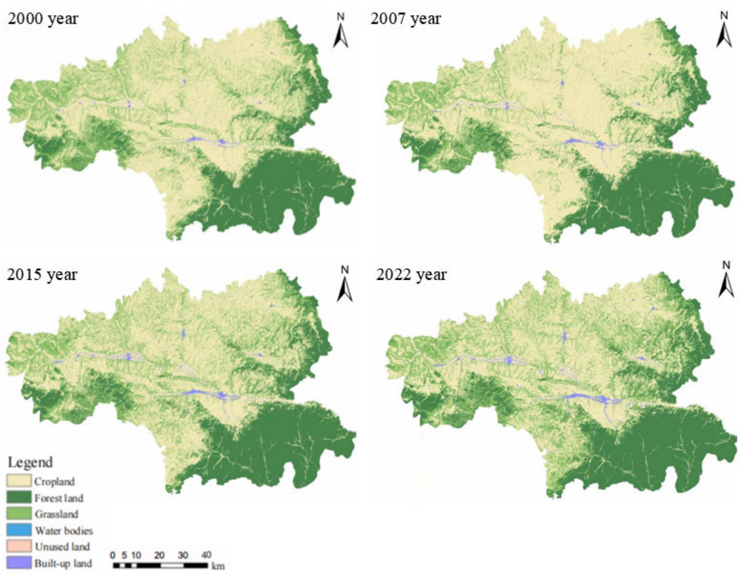

Figure 2. Spatial distribution of land-use types in Tianshui City from 2000 to 2022

Table 1. Areas of different land-use types in Tianshui City from 2000 to 2022 (km²)

Year	Cropland	Forest land	Grassland	Water bodies	Unused land	Built-up land
2000	7142.838	3664.75	3392.049	2.4228	0.2187	74.8386
2007	7849.749	3774.308	2552.484	2.6802	0.0432	97.8516
2015	6512.558	3956.528	3672.631	2.9313	0.1854	132.2829
2022	5717.043	4251.982	4136.625	4.1409	0.9801	166.3452

As shown in Table 1, from 2000 to 2007, all land-use types expanded except grassland and unused land. From 2007 to 2015, grassland increased markedly by 43.88%, while forest land, water bodies, built-up land, and unused land also expanded and cropland declined. From 2015 to 2022, water bodies showed the largest proportional increase, expanding by 41.26%. Forest land, grassland, unused land, and built-up land continued to expand, whereas cropland continued to contract. Over the entire study period, forest land increased by 587.232 km² (16.02%), and grassland increased by

744.576 km² (21.95%), mainly in the northeastern and southwestern parts of the study area. Unused land increased by 0.7614 km² (3.48%), water bodies by 1.7181 km² (70.91%), and built-up land by 91.5066 km² (1.22%). In contrast, cropland decreased by 1,425.795 km², a reduction of 19.96% from its 2000 level.

3.1.2. Changes in land-use dynamic degree

As shown in Table 2, during 2000–2007, built-up land had the highest dynamic degree (4.39%), indicating the fastest rate of change. The dynamic degrees of grassland and unused land were negative, indicating decreases in their areas, whereas those of cropland, forest land, and water bodies were positive, indicating expansion. During 2007–2015, unused land showed the highest dynamic degree (41.15%). The dynamic degree of cropland was −2.13%, whereas those of forest land, grassland, water bodies, and built-up land were 0.60%, 5.49%, 1.17%, and 4.40%, respectively. During 2015–2022, unused land again exhibited the highest dynamic degree (61.23%). Cropland had a negative dynamic degree, whereas the values for forest land, grassland, water bodies, and built-up land were 1.07%, 1.80%, 5.89%, and 3.68%, respectively. Over the entire period from 2000 to 2022, cropland had a negative dynamic degree of −0.91%, whereas all other land-use types had positive values. Unused land exhibited the highest dynamic degree, at 15.82%, indicating increasingly pronounced changes in unused land during the urbanization of Tianshui.

Table 2. Dynamic degree of individual land-use types in Tianshui City from 2000 to 2022 (%)

Period	Dynamic degree of individual land-use types					
	Cropland	Forest land	Grassland	Water bodies	Unused land	Built-up land
2000-2007	1.41%	0.43%	-3.54%	1.52%	-11.46%	4.39%
2007-2015	-2.13%	0.60%	5.49%	1.17%	41.15%	4.40%
2015-2022	-1.75%	1.07%	1.80%	5.89%	61.23%	3.68%
2000-2022	-0.91%	0.73%	1.00%	3.22%	15.82%	5.56%

3.1.3. Characteristics of land-use transitions

To identify the direction, magnitude, and dominant pathways of land-use conversions in Tianshui, land-use data for 2000 and 2022 were spatially overlaid to construct a land-use transition matrix (Table 3). During 2000–2022, conversions occurred mainly among cropland, grassland, and forest land. Grassland recorded the largest net gain, increasing by 744.5763 km². Its total inflow was 1,852.4034 km², of which 1,839.5406 km² originated from cropland, accounting for 99.30%. Spatially, grassland expansion was concentrated mainly in northwestern and southwestern Tianshui. Cropland experienced the largest net loss, decreasing by 1,425.7945 km². Of the cropland converted to other land-use types, 1,839.5406 km² and 173.3994 km² were converted to grassland and forest land, accounting for 87.90% and 8.29% of the total outflow, respectively. Cropland gains were derived mainly from grassland and forest land, which contributed 647.0739 km² and 19.5057 km², respectively. Built-up land increased by a net 91.5066 km². Of its total inflow of 92.2392 km², cropland and grassland contributed 77.5071 km² (84.03%) and 13.9059 km² (15.08%), respectively. Forest land increased by a net 587.2320 km², with most of its inflow originating from grassland and cropland, which contributed 445.8375 km² (72.00%) and 173.3994 km² (28.00%), respectively. Water bodies increased by a net 1.7181 km², with inflows derived mainly from cropland and grassland, whereas unused land underwent limited conversion and showed only minor overall change. Overall, grassland, forest land, built-up land, water bodies, and unused land recorded net gains, whereas cropland was the only land-use type with a substantial net loss.

Table 3. Land-use transition matrix for Tianshui City from 2000 to 2022 (km²)

Area change, 2000–2022	Grassland	Cropland	Built-up land	Forest land	Water bodies	Unused land	Total
Grassland	2284.2216	647.0739	13.9059	445.8375	90.99	0.9999	3392.0487
Cropland	1839.5406	5050.0845	77.5071	173.3994	143.28	0.873	7142.8374
Built-up land	0.0126	0.0405	74.106	0	67.95	0	74.8386
Forest land	12.483	19.5057	0.0171	3632.7429	0.09	0	3664.7496
Water bodies	0.1998	0.3222	0.7758	0.0018	111.78	0.0054	2.4228
Unused land	0.1674	0.0162	0.0333	0	0	0.0018	0.2187
Total	4136.625	5717.043	166.3452	425198.16	4.1409	0.9801	14277.1158

3.1.4. Spatiotemporal evolution of fractional vegetation cover

Fractional vegetation cover (FVC) in Tianshui was estimated for 2000, 2007, 2015, and 2022. Following the classification criteria specified in the Standards for Classification and Grading of Soil Erosion, FVC was divided into five classes: low, relatively low, moderate, relatively high, and high (Table 4).

Table 4. Classification criteria for fractional vegetation cover

Level	Fractional vegetation cover	Vegetation-cover class
1	<30%	Low FVC
2	30%—45%	Relatively low FVC
3	45%—60%	Moderate FVC
4	60%—75%	Relatively high FVC
5	>75%	High FVC

As shown in Fig. 3, FVC exhibited a clear northwest–southeast gradient from 2000 to 2022, with lower values in the northwest and higher values in the southeast. Northwestern Tianshui is located in the loess hilly and gully region of the Loess Plateau, where unfavorable environmental conditions restrict vegetation growth. In contrast, southeastern Tianshui extends into the western Qinling Mountains, where extensive cropland and forest land support higher FVC. Areas of low and relatively low FVC coincided mainly with built-up land and water bodies. Moderate-FVC areas formed transitional zones between low- and high-FVC areas and were located primarily in northern Qin'an County, northwestern Qingshui County, and southwestern Qinzhou District. Relatively high-FVC areas were distributed mainly in southeastern Qinzhou District, the Xiaolongshan forest area of Maiji District, the Guanshan forest–grassland area in eastern Qingshui County and Zhangjiachuan Hui Autonomous County, and the western Qinling forest areas in southern Wushan and Gangu counties. Low-FVC areas generally occurred under unfavorable natural conditions or intensive anthropogenic disturbance. At the county level, Gangu County had relatively low FVC because of its large population and intensive human disturbance, whereas Maiji District had relatively high FVC owing to its extensive forest cover and favorable natural conditions.

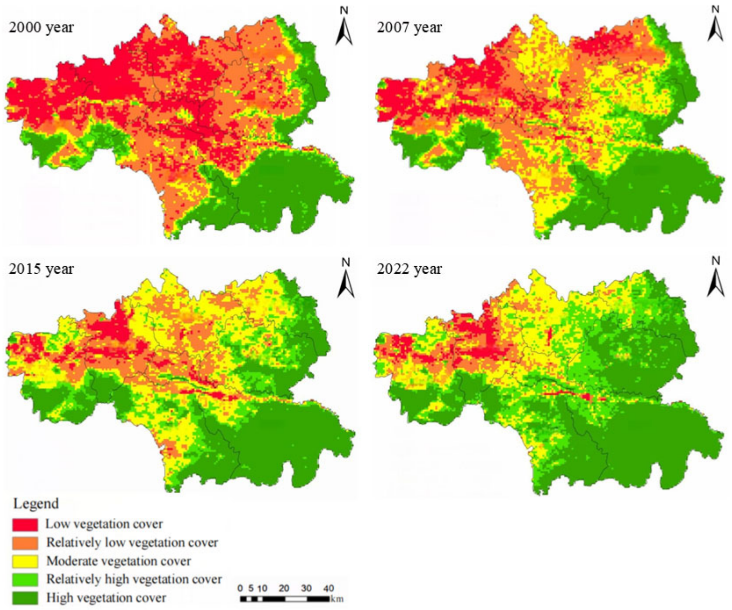

Figure 3. Spatial distribution of fractional vegetation cover classes in Tianshui City from 2000 to 2022.

Table 5 indicated a substantial overall increase in FVC in Tianshui during the study period. This improvement was associated with the implementation of the Grain for Green Program and the Natural Forest Protection Program since 2000, indicating an overall positive trajectory in vegetation cover. During 2000–2022, high-FVC areas accounted for an average of 32.25% of the total area, whereas relatively high-, moderate-, relatively low-, and low-FVC areas accounted for 13%, 19.75%, 23%, and 12%, respectively. The areas of high and relatively high FVC increased progressively by 2,884 km² and 2,186 km², respectively. Moderate-FVC area increased by 2,820 km² from 2000 to 2015 and subsequently decreased by 1,028 km² from 2015 to 2022. By contrast, the areas of relatively low and low FVC declined progressively by 3,551 km² and 3,311 km², respectively.

Table 5. Area (km²) and proportion (%) of the spatial distribution of vegetation cover in Tianshui City from 2000 to 2022

Type	2000		2007		2015		2022	
	Area (km²)	Proportion (%)	Area (km²)	Proportion (%)	Area (km²)	Proportion (%)	Area (km²)	Proportion (%)
Low FVC	3886	27%	1697	12%	769	5%	575	4%
Relatively low FVC	4947	35%	4050	28%	2688	19%	1396	10%
Moderate FVC	1137	8%	3244	23%	3957	28%	2929	20%
Relatively high FVC	907	6%	1430	10%	2000	14%	3093	22%
High FVC	3397	24%	3853	27%	4860	34%	6281	44%

3.1.5. Characteristics of transitions among fractional vegetation cover classes

Table 6 shows that, among the five fractional vegetation cover (FVC) classes, high FVC recorded the largest net gain from 2000 to 2022, increasing by 2,884 km². This increase arose mainly from the conversion of relatively low- and relatively high-FVC areas and coincided with grassland expansion. High FVC also recorded the smallest outflow, at only 32 km². Relatively high FVC received 3,006 km², mainly from low- and relatively low-FVC areas, which contributed

897 km² and 1,806 km², or 30% and 60% of the total inflow, respectively. Moderate FVC received 2,820 km², primarily from low- and relatively low-FVC areas, which contributed 1,335 km² and 1,472 km², or 47.34% and 52.20% of the total inflow, respectively. Relatively low FVC recorded the largest outflow, with 4,569 km² converted to other classes. Of this area, 1,806 km² and 1,472 km² shifted to relatively high and moderate FVC, accounting for 39.53% and 32.22% of the total outflow, respectively. Low FVC lost 3,410 km², mainly through conversion to relatively low and moderate FVC, which received 963 km² and 1,335 km², accounting for 28.24% and 39.15% of the total outflow, respectively. Overall, the areas of high, relatively high, and moderate FVC increased between 2000 and 2022, whereas those of relatively low and low FVC decreased, indicating an overall increase in vegetation cover and improved ecological conditions in Tianshui.

Table 6. Fractional vegetation cover transition matrix for Tianshui City from 2000 to 2022 (km²)

2000	2022					
	Low FVC	Relatively low FVC	Moderate FVC	Relatively high FVC	High FVC	Total
Low FVC	476	963	1335	897	215	3886
Relatively low FVC	77	378	1472	1806	1214	4947
Moderate FVC	18	49	109	272	689	1137
Relatively high FVC	4	6	12	87	798	907
High FVC	0	0	1	31	3365	3397
Total	575	1396	2929	3093	6281	14274

3.1.6. Indicator Selection and Model Construction

Using spatial overlay analysis in ArcGIS 10.7, FVC data were overlaid with land-use data, and the Tabulate Intersection tool was used to quantify FVC for each land-use type. As shown in Fig. 4, FVC differed substantially among land-use types and exhibited distinct temporal patterns. Forest land consistently showed the highest FVC, reflecting its relatively continuous vegetation cover, whereas unused land and built-up land generally had lower values. FVC in cropland increased steadily from 2000 to 2022, indicating a continuous improvement in vegetation cover. Forest-land FVC decreased between 2000 and 2007, changed only slightly from 2007 to 2015, and increased markedly after 2015. FVC in grassland and water bodies increased during 2000–2015 but declined from 2015 to 2022. Unused land showed an initial increase followed by a continuous decrease, whereas built-up land fluctuated only slightly throughout the study period. Overall, the temporal evolution of FVC varied among land-use types, indicating that vegetation-cover changes were closely associated with differences in land-use characteristics and their transformations.

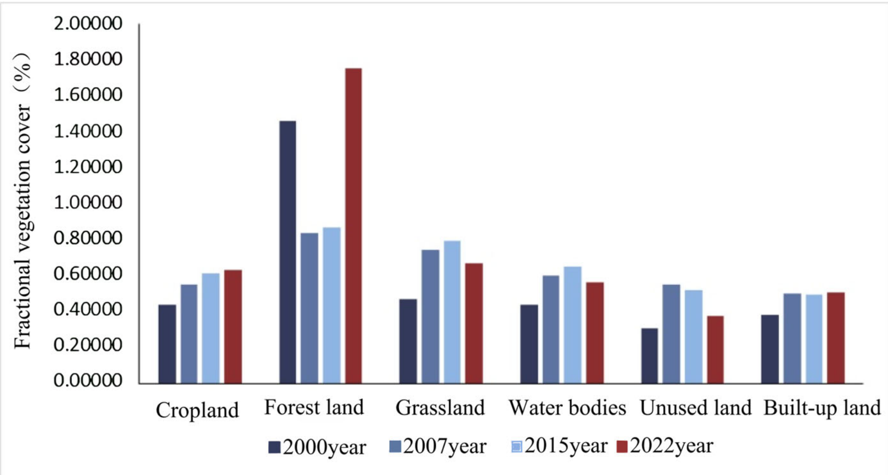

Figure 4. Changes in fractional vegetation cover under different land-use types in Tianshui City from 2000 to 2022

4. Discussion

The results showed that land-use patterns in Tianshui changed markedly between 2000 and 2022. Cropland declined continuously, whereas forest land, grassland, and built-up land generally expanded. Conversions occurred mainly among cropland, forest land, and grassland, reflecting the combined influence of ecological restoration, agricultural land-use adjustment, and urban expansion. The conversion of cropland to forest land and grassland may have been associated with the Grain for Green Program, the Natural Forest Protection Program, and soil erosion control projects, whereas built-up land expansion increased spatial competition between urban development and cropland conservation. Over the same period, fractional vegetation cover (FVC) generally improved, as low-FVC areas gradually transitioned to moderate- and high-FVC classes, with higher values in the southeast and lower values in the northwest. These patterns suggest that vegetation change was shaped by land-use adjustment together with topography, hydrothermal conditions, initial vegetation conditions, and human disturbance. FVC differed markedly among land-use types, being generally higher in forest land and grassland and lower in unused land and built-up land. However, within-class variation may also reflect differences in precipitation, cropping systems, stand structure, grazing intensity, and land management. Land-use change was therefore closely associated with vegetation-cover dynamics, although transition matrices and spatial overlay analyses alone cannot establish direct causality. Future land management should strengthen cropland protection, limit unregulated built-up land expansion, and implement region-specific ecological restoration according to local environmental carrying capacity. Future research should integrate continuous annual, high-resolution remote-sensing data with climatic, demographic, and ecological-restoration variables to identify the mechanisms driving land-use and vegetation-cover changes.

References

[1] Turner, B. L., II, Lambin, E. F., & Reenberg, A. (2007). The emergence of land change science for global environmental change and sustainability. *Proceedings of the National Academy of Sciences*, 104(52), 20666–20671. https://doi.org/10.1073/pnas.0704119104

[2] Foley, J. A., DeFries, R., Asner, G. P., Barford, C., Bonan, G., Carpenter, S. R., Chapin, F. S., Coe, M. T., Daily, G. C., Gibbs, H. K., Helkowski, J. H., Holloway, T., Howard, E. A., Kucharik, C. J., Monfreda, C., Patz, J. A., Prentice, I. C., Ramankutty, N., & Snyder, P. K. (2005). Global consequences of land use. *Science*, 309(5734), 570–574. https://doi.org/10.1126/science.1111772

[3] Meyfroidt, P., de Bremond, A., Ryan, C. M., Archer, E., Aspinall, R., Chhabra, A., Câmara, G., Corbera, E., DeFries, R., Díaz, S., Dong, J., Ellis, E. C., Erb, K. H., Fisher, J. A., Garrett, R. D., Golubiewski, N. E., Grau, H. R., Grove, J. M., Haberl, H., … zu Ermgassen, E. K. H. J. (2022). Ten facts about land systems for sustainability. *Proceedings of the National Academy of Sciences*, 119(7), e2109217118. https://doi.org/10.1073/pnas.2109217118

[4] Lambin, E. F., Turner, B. L., II, Geist, H. J., Agbola, S. B., Angelsen, A., Bruce, J. W., Coomes, O. T., Dirzo, R., Fischer, G., Folke, C., George, P. S., Homewood, K., Imbernon, J., Leemans, R., Li, X., Moran, E. F., Mortimore, M., Ramakrishnan, P. S., Richards, J. F., … Xu, J. (2001). The causes of land-use and land-cover change: Moving beyond the myths. *Global Environmental Change*, 11(4), 261–269. https://doi.org/10.1016/S0959-3780(01)00007-3

[5] Zhang, L., Yang, L., Zohner, C. M., Crowther, T. W., Li, M., Shen, F., Guo, M., Qin, J., Yao, L., & Zhou, C. (2022). Direct and indirect impacts of urbanization on vegetation growth across the world's cities. *Science Advances*, 8(27), eabo0095. https://doi.org/10.1126/sciadv.abo0095

[6] Piao, S., Wang, X., Park, T., Chen, C., Lian, X., He, Y., Bjerke, J. W., Chen, A., Ciais, P., Tømmervik, H., Nemani, R. R., & Myneni, R. B. (2020). Characteristics, drivers and feedbacks of global greening. *Nature Reviews Earth & Environment*, 1(1), 14–27. https://doi.org/10.1038/s43017-019-0001-x

[7] Carlson, T. N., & Ripley, D. A. (1997). On the relation between NDVI, fractional vegetation cover, and leaf area index. *Remote Sensing of Environment*, 62(3), 241–252. https://doi.org/10.1016/S0034-4257(97)00104-1

[8] Gao, L., Wang, X., Johnson, B. A., Tian, Q., Wang, Y., Verrelst, J., Mu, X., & Gu, X. (2020). Remote sensing algorithms for estimation of fractional vegetation cover using pure vegetation index values: A review. *ISPRS Journal of Photogrammetry and Remote Sensing*, 159, 364–377. https://doi.org/10.1016/j.isprsjprs.2019.11.018

[9] Mu, X., Yang, Y., Xu, H., Guo, Y., Lai, Y., McVicar, T. R., Xie, D., & Yan, G. (2024). Improvement of NDVI mixture model for fractional vegetation cover estimation with consideration of shaded vegetation and soil components. *Remote Sensing of Environment*, 314, 114409. https://doi.org/10.1016/j.rse.2024.114409

[10] Song, X.-P., Hansen, M. C., Stehman, S. V., Potapov, P. V., Tyukavina, A., Vermote, E. F., & Townshend, J. R. (2018). Global land change from 1982 to 2016. *Nature*, 560(7720), 639–643. https://doi.org/10.1038/s41586-018-0411-9

[11] Weng, Q., Lu, D., & Schubring, J. (2004). Estimation of land surface temperature–vegetation abundance relationship for urban heat island studies. *Remote Sensing of Environment*, 89(4), 467–483. https://doi.org/10.1016/j.rse.2003.11.005

[12] Chen, C., Park, T., Wang, X., Piao, S., Xu, B., Chaturvedi, R. K., Fuchs, R., Brovkin, V., Ciais, P., Fensholt, R., Tømmervik, H., Bala, G., Zhu, Z., Nemani, R. R., & Myneni, R. B. (2019). China and India lead in greening of the world through land-use management. *Nature Sustainability*, 2(2), 122–129. https://doi.org/10.1038/s41893-019-0220-7

[13] Feng, X., Fu, B., Piao, S., Wang, S., Ciais, P., Zeng, Z., Lü, Y., Zeng, Y., Li, Y., Jiang, X., & Wu, B. (2016). Revegetation in China's Loess Plateau is approaching sustainable water resource limits. *Nature Climate Change*, 6(11), 1019–1022. https://doi.org/10.1038/nclimate3092

[14] Peng, J., Fan, Z., Wu, D., Zhuang, J., Dai, F., Chen, W., & Zhao, C. (2015). Heavy rainfall triggered loess–mudstone landslide and subsequent debris flow in Tianshui, China. *Engineering Geology*, 186, 79–90. https://doi.org/10.1016/j.enggeo.2014.08.015

[15] Zhang, Z.-L., Wang, T., & Wu, S.-R. (2020). Distribution and features of landslides in the Tianshui Basin, Northwest China. *Journal of Mountain Science*, 17(3), 686–708. https://doi.org/10.1007/s11629-019-5595-4

[16] Pontius, R. G., Jr., Huang, J., Jiang, W., Khallaghi, S., Lin, Y., Liu, J., Quan, B., & Ye, S. (2017). Rules to write mathematics to clarify metrics such as the land use dynamic degrees. *Landscape Ecology*, 32(12), 2249–2260. https://doi.org/10.1007/s10980-017-0584-x

[17] Zhou, K., Wang, X., Wang, Z., & Hu, Y. (2022). Systematicity and stability analysis of land use change—Taking Jinan, China, as an example. *Land*, 11(7), 1045. https://doi.org/10.3390/land11071045